## RESEARCH ARTICLE



# Large contribution of woody plant expansion to recent vegetative greening of the Northern Great Plains

Bryce Currey<sup>1</sup> David B. McWethy<sup>2</sup> Nicholas R. Fox<sup>1</sup> E. N. Jack Brookshire<sup>1</sup>

<sup>1</sup>Department of Land Resources and Environmental Sciences, Montana State University, Bozeman, Montana, USA

<sup>2</sup>Department of Earth Sciences, Montana State University, Bozeman, Montana, USA

#### Correspondence

Bryce Currey, Department of Land Resources and Environmental Sciences, Montana State University, Bozeman, Montana, USA.

Email: brycecurrey93@gmail.com

#### **Funding information**

U.S. Bureau of Land Management; Montana Agricultural Experiment Station; National Science Foundation

Handling Editor: Simon Scheiter

#### Abstract

Aim: Extensive portions of high-latitude grasslands worldwide have recently experienced increased vegetative productivity (i.e., greening) and have undergone a rapid transition towards woody plant dominance via the process of woody plant expansion (WPE). This raises the underlying question: To what degree are WPE and greening spatiotemporally linked? Given that these vegetative changes are predicted to continue, we seek to understand how recent changes in vegetation extent and productivity have interacted under recent climate change and anthropogenic disturbance to provide insights surrounding the future trajectory of temperate grasslands broadly.

Location: Northern Great Plains (NGP), North America.

Taxon: Woody plants.

Methods: Greening was measured as the significant increase in three metrics between 2000 and 2019: leaf area index (LAI), annual maximum normalized difference vegetative index (NDVI) and annual mean NDVI. WPE was measured as the significant proportional increase in percent tree cover change between 2000 and 2019 in grasslands. We then examined these variables across a host of 26 potential driving variables.

Results: We show that average proportional greening increased by 0.2-1.3% year<sup>-1</sup> (depending on metric), and proportional WPE increased by 6.9% year<sup>-1</sup> since 2000 across the NGP. Both changes are largely driven by the absence of wildfire and changing climate. Furthermore, WPE was spatially coherent and positively associated with a large component of recent greening, as revealed by their coupling across 34.1%-40.6% of grassland area and as evidenced by the 9.7%-19.7% of the variability in greening explained by WPE.

Main conclusions: WPE and greening are spatiotemporally coupled across large portions of the NGP. Under continued climate change and wildfire suppression, WPE and greening are likely to continue across large swathes of grasslands globally. Furthermore, our results show that using a single greening metric may be insufficient to capture the large-scale vegetative changes such as the expansion of woody vegetation.

#### KEYWORDS

greening, leaf area index, normalized difference vegetation index, Northern Great Plains, temperate grasslands, woody plant encroachment, woody plant expansion

Strapline: We find that large climatic changes and the absence of fire have driven large woody plant expansion in the Northern Great Plains, and that this expansion of woody cover comprise a large portion of recent vegetative greening across this temperate grassland ecosystem.

## 1 | INTRODUCTION

Globally, large areas of temperate grasslands are undergoing vegetative shifts towards an increased prevalence of shrubs and trees, hereafter referred to as "woody plant expansion" (WPE; Barger et al., 2011; Criado et al., 2020; Stevens et al., 2017). Simultaneously, large increases in vegetative photosynthetic activity or productivity ("greening") have been documented across temperate grasslands (Chen, Park, et al., 2019; Chen, Parton, et al., 2019). Independently, these two vegetative changes have large consequences for grassland biophysical processes, biodiversity and biogeochemistry (Andersen & Steidl, 2019; Brookshire et al., 2020; Eldridge et al., 2011; Ratajczak et al., 2012; Welti et al., 2020). Furthermore, dynamic global vegetation models (DGVMs) have projected that both changes will continue in the future (Hufkens et al., 2016; Klemm et al., 2020; Reeves et al., 2014; Shafer et al., 2015). Increased woody plant cover has been hypothesized to be responsible for recent greening trends across grassland and savanna ecosystems (Chen, Park, et al., 2019; Deng et al., 2021; Xiao & Moody, 2005), but to what extent WPE contributes to greening and to what degree these two phenomena are spatiotemporally coupled in extent and driving mechanisms at fine resolution remains unresolved.

The most common approaches for measuring greening use the normalized difference vegetation index (NDVI) or leaf area index (LAI; Piao et al., 2020). LAI provides information on photosynthetic surface area (i.e., canopy structural complexity), whereas NDVI is biomassindependent and a more direct proxy of photosynthetic activity. NDVI is often measured using the maximum value across a time series (peak NDVI) or the mean value from a time series (mean NDVI). Peak NDVI highlights the maximum photosynthetic active radiation and subsequent maximum vegetative productivity (Myneni et al., 1995), whereas mean NDVI integrates annual vegetative production. Peak NDVI is often preferred over other metrics as it is best at minimizing error from cloud, reflectance, shadow and aerosol effects (Myneni et al., 1995). However, changes in peak NDVI may be insufficient to distinguish between WPE dynamics and background greenness if the expanding shrubs and trees are primarily evergreen (thus, maintain a relatively constant NDVI year-round). In this case, mean annual NDVI would capture the elongated NDVI signal across the year under WPE, whereas the maximum values may not change. Furthermore, both NDVI metrics may be inadequate compared with LAI, which captures the higher canopy complexity of trees than herbaceous vegetation. Although LAI and aboveground net primary productivity (ANPP) have both been associated with higher woody cover (Barger et al., 2011; Knapp et al., 2008), and NDVI and ANPP have been linked at coarse scales (Reeves et al., 2020), how these associations and their underlying assumptions apply to WPE is uncertain.

That WPE and greening are coupled at local scales is reasonable, but how both phenomena and their drivers are linked in space and across time at the landscape scale remains largely unknown. WPE and greening are most commonly attributed to increasing CO<sub>2</sub>, changing climate, and shifts in disturbance regimes (Archer et al., 2017; Zhu et al., 2016), yet disentangling these drivers and their interactions have

proven challenging. For example, elevated CO<sub>2</sub> can promote greening via directly stimulating photosynthesis and indirectly via increased water- and/or nutrient-use efficiency (WUE/NUE), but the strength of this effect can vary greatly among plant functional types (Feng et al., 2015; Terrer et al., 2019) and may be constrained by climate and nutrient availability (Brookshire et al., 2020; Frank et al., 2015). Precipitation dictates the bioclimatic limits of woody cover (Scholtz et al., 2018), and higher temperatures are strongly correlated with increased shrub cover (Criado et al., 2020). However, increases in temperature and precipitation also drive enhanced vegetative productivity, particularly in semi-arid environments, irrespective of WPE (Knapp et al., 2017; Zhu et al., 2016). Similarly, fire and herbivory can provide a check on expanding tree cover (Fuhlendorf et al., 2009), yet these disturbances may have negative, neutral or positive effects on greening (Frank et al., 1998; Geremia et al., 2019). Therefore, it is crucial to disentangle regionally specific climatic and disturbance drivers of WPE and greening at fine spatial and temporal resolution to understand the degree to which WPE contributes to greening.

We examined potential synchrony between WPE and greening across the Northern Great Plains (NGP) of North America. The current extent of WPE across the NGP has not been quantified, despite anecdotal (Symstad & Leis, 2017) and historical photographic evidence (Phillips et al., 1963) of WPE. Peak photosynthetic productivity has increased in recent decades (Brookshire et al., 2020) and is predicted to continue in the future (Hufkens et al., 2016; Reeves et al., 2014). In addition, the climate of the NGP is predicted to get warmer and wetter (Conant et al., 2018; Polley et al., 2013), and DGVMs have projected extensive climate-driven increases in woody cover across NGP grasslands in the future (Klemm et al., 2020; Shafer et al., 2015). Importantly, these simulations have not been constrained by historical observations of WPE. It is essential to disentangle the recent trends and drivers of the potentially synchronous vegetative changes to benchmark and constrain these interactions for simulating future vegetative changes accurately.

Here, we ask: (1) What is the magnitude and extent of WPE and greening across the NGP? (2) What are the drivers of WPE and greening across large topographic and climate ranges? (3) To what degree are WPE and productivity synchronous across the land-scape and through time? We use products from NASA's Moderate-Resolution Imaging Spectroradiometer (MODIS) to explore changes in peak NDVI, mean NDVI, LAI and percent tree cover between 2000 and 2019. We examine these vegetative changes against 26 possible climate, physical and disturbance driving variables using a combination of random forest algorithms and linear regression.

# 2 | MATERIALS AND METHODS

#### 2.1 | Study area

The NGP (as defined in this study) covers roughly 744,000 km<sup>2</sup>, spans 15 degrees of longitude and 11 degrees of latitude (97.85–112.65 W, 40.69–50.03 N), and covers portions of five U.S. states

and two Canadian provinces (Figure 1). Mean annual precipitation (MAP) spans a wide gradient from 235 mm in the Northcentral-western regions to 1214 mm in the Southeastern and mountainous areas, and mean annual temperature (MAT) generally decreases with increasing latitude from 10.4 to 0.8 °C. Elevation in the NGP varies from 368 to >2500 m above the sea level.

According to the 2010 North American Land Change Monitoring System (NALCMS) 30 m landcover dataset, 54.8% of the NGP is grassland, 28.4% is cropland, 7.6% is shrubland, 3% is forested (either deciduous, needleleaf, or mixed), and 6.2% is other (i.e., urban, water, and wetland; Figure 1). For our research, we restricted our analyses to the combined grassland and shrubland layers (hereafter "grasslands"; 62.3% or ~463,000 km² of the NGP) as we were only interested in tree cover changes in non-forested areas. Across most of our study area, the primary trees implicated in WPE are *Pinus ponderosa* Douglas ex C. Lawson and numerous *Juniperus* species, including *J. horizontalis* Moench, *J. Communis* Linnæus, *J. scopulorum* Sarg. and *J. virginia* Linnæus (Brown & Sieg, 1999; Symstad & Leis, 2017). Some deciduous aspen (*Populus tremuloides* Michx) expansion has also been documented in the northern regions (Köchy & Wilson, 2001).



FIGURE 1 Study area schematic for the northern Great Plains (NGP). (a) The extent of the NGP within North America. Dark grey indicates the five states and two providences partially occupied by the NGP. (b) Seven land cover types within the NGP. Grassland and shrubland layers were combined under the umbrella term 'grassland.' (c) The 'grassland' composite layer, covering roughly two-thirds of the study area. The largest non-grassland area is comprised of cropland

## 2.2 | Data collection

All variables and their respective statistics can be found in Table \$1.1 and are displayed in Figures \$1.1–1.5. Table \$1.2 contains information about the merged soils dataset. All analyses were conducted using R 4.0.3. For a list of all packages used and the respective citations, see Table \$3.1, and for a list of all datasets used, see Table \$3.2. Finally, all data and analyses are publicly available at https://doi.org/10.5061/dryad.z08kprrdj.

#### 2.2.1 | Tree cover, NDVI and LAI

We examined a two-decade time series (2000–2019) of WPE, NDVI and LAI data. Peak and mean NDVI were calculated from NASA's MODIS Vegetation Indices 16-day product (Version 6) at a 500 m spatial scale. LAI was calculated as the mean yearly value from the MODIS 8-day LAI/FPAR product (V6) at a 500 m resolution. WPE is defined in this study as grassland pixels significantly increasing in percent tree cover. Percent tree cover was obtained from the MODIS Vegetation Continuous Fields 16-day product (V6) at a 250 m spatial scale and resampled using the median pixel value to 500 m. This product implements decision tree theory on a host of auxiliary variables (e.g., both MODIS and LANDSAT bands), which allows the algorithm to capture vegetation cover at lower percent tree cover values, although this product has been found to underestimate tree cover (Adzhar et al., 2022).

To determine significant (p < 0.05) changes in NDVI, LAI and tree cover over time, we used a two-sided Mann-Kendal trend test across the 20-year period. Only for pixels showing significant changes, percent change was calculated relative to initial values, and the inner 99% of the data was kept, removing exceptionally large (e.g.,  $\pm 4\sigma$ ) outliers. A uniform 1% was added across all tree cover values so that an increase from zero would not yield an infinite result but was subtracted for magnitude calculations and mapping. We also created a 'Greening Index' to examine areas that were increasing in all three greening metrics. This was done by scaling each metric between zero and one and taking the sum, excluding all areas not greening in all three metrics. As such, the theoretical maximum value of the greening index is three, and values lower than three indicate some degree of greening from all metrics. For greening and WPE statistics, we calculated the geometric mean and standard deviation (SD) as the distributions were highly right-skewed.

#### 2.2.2 | Climate data

Climate data were obtained from NASA's *Daymet* (1 km resolution resampled to 500 m) gridded daily weather estimates. We determined the difference between the recent (2000–2019) and historical (1980–1999) periods for MAP, MAT and mean seasonal climatologies. Relevant seasons were defined as spring (April, May, June;

AMJ), summer (July, August, September; JAS) and winter (December, January, February, March; DJFM). We estimated precipitation variability by calculating the temporal coefficient of variation (CV) of MAP over the recent period. Finally, we included annual growing degree days (AGDD) and change in AGDD using a base temperature of 10°C at 1 km resolution data from the Coupled Model Intercomparison Project (Phase 5; CMIP5).

# 2.2.3 | Physical and disturbance variables

To examine the effect of topography, we calculated elevation, slope, aspect and roughness from the Shuttle Radar Topography Mission digital elevation model dataset at 30 m resolution. Roughness is calculated as the difference between the maximum and minimum elevation across the cell and the eight neighbouring cells (i.e., larger values indicate rougher terrain). To examine the four cardinal directions of the aspect as continuous variables, we calculated the sine and cosine of aspect (in radians) to examine the "northness" and "eastness," respectively. Soils were obtained from the National Resource Conservation Service for soils within the United States and from the National Soils Database of Canada for Canadian soils and merged at the generalized order to create seven soil classifications.

We examined three disturbance variables: nitrogen (N) deposition, cattle per km<sup>2</sup> (a proxy for herbivory) and burned area. N deposition (kg N ha<sup>-1</sup> year<sup>-1</sup>) was obtained from the 1993 global product. Cattle per km<sup>2</sup> was obtained for 2010 from the areal-weighted cattle density global product. Finally, total burned area across the study period was obtained from MODIS and was converted into a binary variable of burned/unburned.

# 2.3 | Random forest and statistical analyses

We examined the variable importance metric from random forest models to determine the relative importance of each climate, topographic and disturbance variable on greening and tree cover changes. Each variable's relative importance is calculated by randomly permutating the data to induce randomness to each variable and comparing these simulations to the observation-driven simulations (known as 'decreased accuracy'). The most significant variables have the largest differences between observation-driven versus randomly permutated runs. The error rate of random forest models is calculated as the average of all individual trees' misclassification rates across the forest. Before modelling, feature selection determined only the aspect variables ('northness' and 'eastness') non-relevant and were thus removed from all analyses. We examined the relative importance of all 24 remaining drivers of LAI change, peak and mean NDVI change, tree cover change, and 2019 tree cover. We also examined the drivers of 2000 tree cover for variables with historical data (1980–1999, n = 15). We also assumed constant cattle density, N deposition, and soil type across time. Finally, we calculated

the variance explained by the predictor variables for all models (i.e., pseudo- $R^2$ ). All variables were resampled using median values to the resolution of the greening and tree cover variables (500 m resolution), on which we used 500 classification trees and four variables at each candidate node. These analyses were performed on the Hyalite High-Performance Computing System operated by University Information Technology Research Cyberinfrastructure at the Montana State University.

Because random forest models cannot determine how individual variables interact with the response variables (i.e., the relationship's direction), we examined all 24 variable's responses against WPE, peak NDVI, mean NDVI and LAI using ordinary least squares (OLS) regression models. Before modelling, all variables were standardized (z-score) to examine the effect size on a uniform scale. Effect sizes (slopes from the bivariate OLS models) were combined with the random forest rank importance analysis to examine each variable's importance score and direction concurrently. As such, a higher variable rank indicates higher importance, and a larger z-score indicates a steeper directional slope. It should be noted that a steep relationship (z-score far from the zero line) does not necessitate high variable importance, nor does higher rank importance necessitate a steep slope. For instance, a high importance value but a small z-score indicates a strong spatial coupling but a less steep relationship.

Similarly, we conducted bivariate analyses examining all greening metrics versus tree cover change to examine the variance explained within each greening variable by WPE. We then examined the correlation of WPE and greening variables in two ways: first, we examined each variable's spatial correlation using Tiøstheim's coefficient (A) and, second, we examined Spearman's rank correlation ( $\rho$ ) between the drivers of each response variable (both bounded between 1 and -1). Tiøstheim's coefficient examines the spatial similarity of the response variables, whereas Spearman's coefficient examined the correlation in both z-score and importance of all 24 driving variables of each response variable. Said in another way, Tjøstheim's A examines the degree of co-occurrence, whereas Spearman's  $\rho$  examines the similarity between each vegetative change's driving variables. For the rank correlation analysis between tree cover in the year 2000 and other response variables, we only examined the correlation between the 15 variables used in the 2000 tree cover random forest model.

## 3 | RESULTS

#### 3.1 | Climate, topography and disturbance

#### 3.1.1 | Climate

Recent (2000–2019) MAP increased by 24.5 mm on average over the entire study area compared with the 1980–1999 climatology (Table S1.1 and Figure S1.2) but was regionally heterogeneous. For instance, some areas experienced large declines (decreased <100 mm; primarily in the northern and central regions), yet others

experienced substantial increases (increased >200 mm; primarily in the southern region). The greatest seasonal precipitation increases were in the spring, with winter and summer mean precipitation barely changing on average. MAT also increased on average by 0.1°C (Table S1.1 and Figure S1.3), with the largest average increases in the summer months (~0.7°C). Consequently, AGDD increased across the entirety of the NGP, with the largest increases in the southwestern areas (Figure S1.4).

## 3.1.2 | Disturbance

Over the 20-year study period, ~2.7% of grassland pixels experienced fire (0.135% probability  $yr^{-1}$  across all pixels), translating to ~20,000 km² of burned area (Table S1.1 and Figure S1.5). N deposition across the region was relatively homogenous after being upscaled yet with an evident east-west gradient from a high of 7.4 to a

TABLE 1 Vegetative change metric statistics for NGP grasslands. Inc is the fraction of total area undergoing respective vegetative increase, decrease (Dec) represents the fraction decreasing.  $\bar{x}_{\rm inc}$  (sd) is the geometric average (geometric sd) magnitude of increases in the respective increasing proportion.  $\bar{x}_{\rm dec}$  (sd) is the geometric average (geometric sd) magnitude of decreases in the respective decreasing proportion

	Proportion of NGP grasslands	Inc	$\bar{x}_{inc}(SD)$	Dec	$\bar{x}_{dec}(SD)$
Tree Cover $\Delta$	48.0	46.8	137.8 (2.3)	1.2	-17.7 (3.5)
LAI Δ	77.6	76.0	26.8 (2.1)	1.6	-3.9 (4.3)
Peak NDVI $\Delta$	63.0	62.7	9.9 (1.7)	0.3	-1.9 (4.6)
Mean NDVI $\Delta$	58.9	57.3	4.2 (1.9)	1.6	-1.7 (4.1)

low of 1.8 kg N ha<sup>-1</sup> year<sup>-1</sup>, and well within the range of in situ studies from the region (Symstad et al., 2019). Finally, the average distribution of cattle across the NGP was 12.5 head km<sup>-2</sup>, but regions in the southern NGP showed densities as high as ~137 head km<sup>-2</sup>.

# 3.2 | Greening and WPE

# 3.2.1 | Extent of greening

We document extensive but variable greening across most NGP grasslands (Table 1; Figure 2). LAI increases were the most extensive, occurring across 76.0% of grassland pixels. LAI-based greening also had the largest proportional 20-year changes of 26.8 (2.1)% on average, or ~1.3% year $^{-1}$ . Next, peak NDVI increased significantly across 62.7% of grasslands, with a magnitude of 9.9 (1.7)%, or ~0.5% year $^{-1}$ . Finally, mean NDVI increased in over half (57.3%) of grassland pixels by 4.2 (1.9)%, or ~0.2% year $^{-1}$ . Synchronous increases in all three metrics (i.e., the extent of the greening index) occurred across 30.6% of NGP grassland area, and all three metrics had a moderately high Tjøstheim's coefficient ( $A \ge 0.42$ ; Table S2.1). We note slightly higher greening in shrubland versus grassland pixels, although the magnitude of changes was similar (Table S2.2).

# 3.2.2 | Driving variables of greening

All random forest classification models for greening performed exceptionally well with error rates for LAI, peak NDVI and mean NDVI changes of 1.43%, 0.44% and 1.49%, respectively. Despite strong model performance, the 24 predictor variables only explained 32.7%, 24.4% and 53.9% of each greening metric's respective variance.

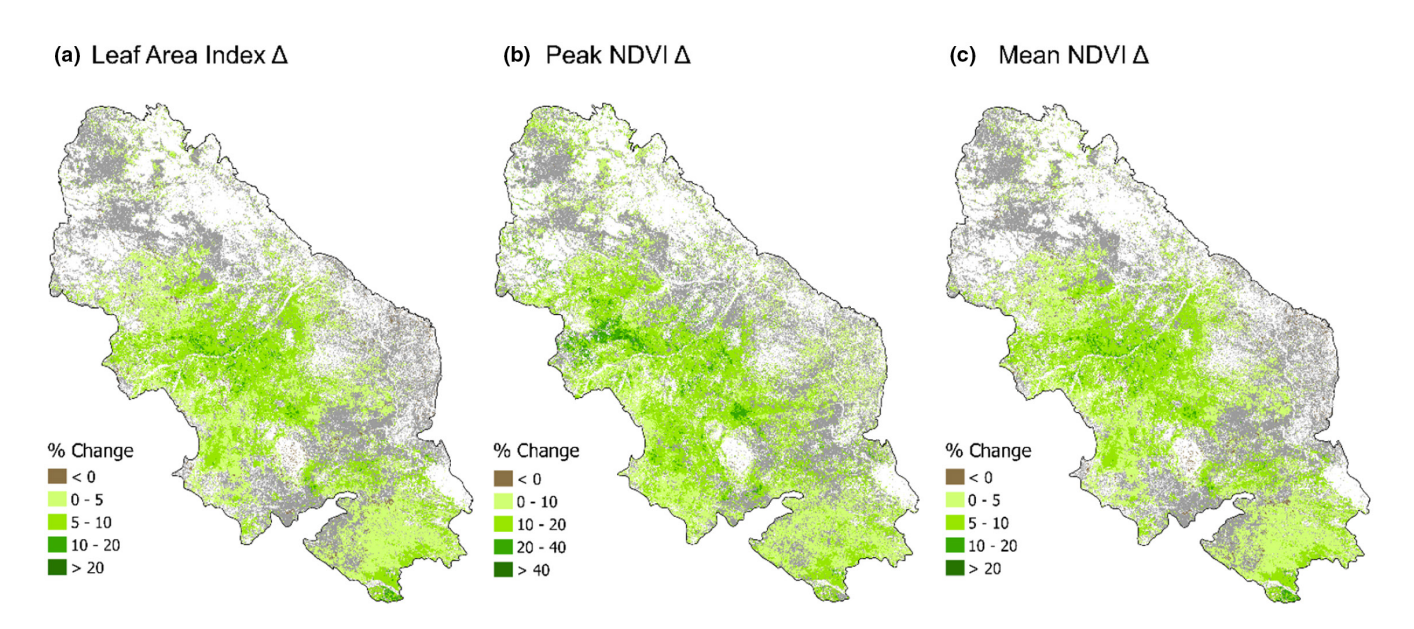


FIGURE 2 NGP grassland (shaded grey) proportional greening changes from 2000 to 2019 measured as (a) LAI changes, (b) peak NDVI changes, and (c) mean NDVI changes. White areas represent non-grasslands (i.e., forested, cropland, urban, wetland)

Roughness, slope and elevation were negatively associated with increasing LAI (Figure 3a), indicating that LAI-based greening was largest on smooth, flat topographies. High precipitation variability and absence of fire were also strong predictors. Precipitation drivers of LAI greening were seasonally dependent, although increasing MAP was correlated with increasing LAI. Warming summer temperatures were also positively associated with LAI. For peak NDVI (Figure 3b), greening was positively associated with higher precipitation variability and increasing precipitation (save for winter precipitation). Peak NDVI-based greening was strongly associated with smoother topographies and low cattle density. Interestingly, fire was a poor predictor of peak NDVI-based greening. Conversely, the absence of fire was the strongest predictor of mean NDVI increases (Figure 3c). The highest mean NDVI-based greening was associated with smoother topographies and lower elevations. Finally, year-round wetting, albeit variably, and warming temperatures were strong driving variables of higher mean NDVI greening.

Overall, smoother topographies and the absence of fire (save for peak NDVI) were strong predictors of greening. Seasonally dependent changes in precipitation and temperature were apparent, in which warmer and wetter summers, but cooler and drier winters, led to the highest proportional greening, apart from mean NDVI, which was driven by a year-round increase in precipitation. Higher precipitation variability was also associated with the largest proportional changes of all three metrics. Lower cattle densities (i.e., herbivory) were a moderately strong predictor of NDVI-based greening. N deposition, AGDD, baseline climatology and soil variables were less important driving variables for greening metrics. Despite climatic differences, the driving variables of all greening metrics had high Spearman correlations ( $\rho \ge 0.75$ ; Table S2.1).

## 3.2.3 | Extent of tree cover and WPE

Initial (year 2000) median percent tree cover in NGP grasslands was 1.6% and generally very low across the entire region (Table 2, Figure 4a). Nonetheless, close to half (46.8%) of grassland pixels observed a significant increase in percent tree cover over the two decades (Table 1, Figure 4b). As a result, proportional tree cover changes were large, with the average increase at 137.8 (2.3)%, or ~6.9% year<sup>-1</sup>, compared to tree cover in 2000. These large proportional changes increased the median percent tree cover to 3.4% by 2019, a 1.8% cover increase over the 20-year period (0.09% cover year<sup>-1</sup>; Figure S2.1a). Interestingly, the inner quartile range in 2000

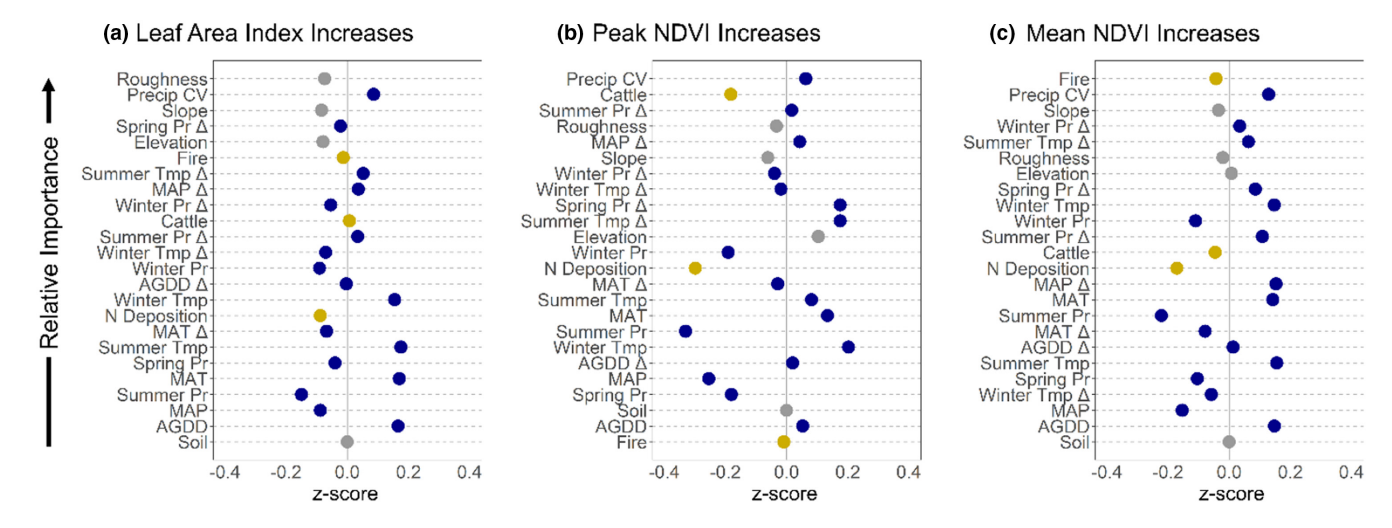


FIGURE 3 Relative importance from random forest models in descending order of importance for the three greening indices: (a) LAI increases, (b) peak NDVI increases, and (c) mean NDVI increases. On the x-axis, standardized (z-score) effect size coefficients from ordinary least-squares regression. Positive values indicate a significant positive relationship with the greening metric; negative values indicate a significant negative relationship. Dots farther away from the zero line indicate a steeper slope. The fire product was converted to a numeric variable, with positive one indicating fire presence and zero indicating absence. Soil is on the zero line as it was kept a categorical variable. Grey circles signify topographic variables, gold circles signify disturbance variables, and blue circles signify climate variables

	Year 2	Year 2000			Year 2019			
	Q1	$\bar{x}$	Q3	IQR	Q1	$\bar{x}$	Q3	IQR
Tree Cover	1.0	1.6	2.7	1.7	1.8	3.4	6.5	4.7
LAI	0.28	0.38	0.51	0.23	0.48	0.50	0.65	0.17
Peak NDVI	0.37	0.46	0.58	0.21	0.51	0.60	0.71	0.20
Mean NDVI	0.22	0.26	0.31	0.09	0.26	0.30	0.34	0.08

TABLE 2 Vegetative metrics for NGP grasslands. Q1 and Q3 are the inner quartiles for the respective vegetative metric, IQR is the inner quartile range, and  $\bar{x}$  is the geometric average

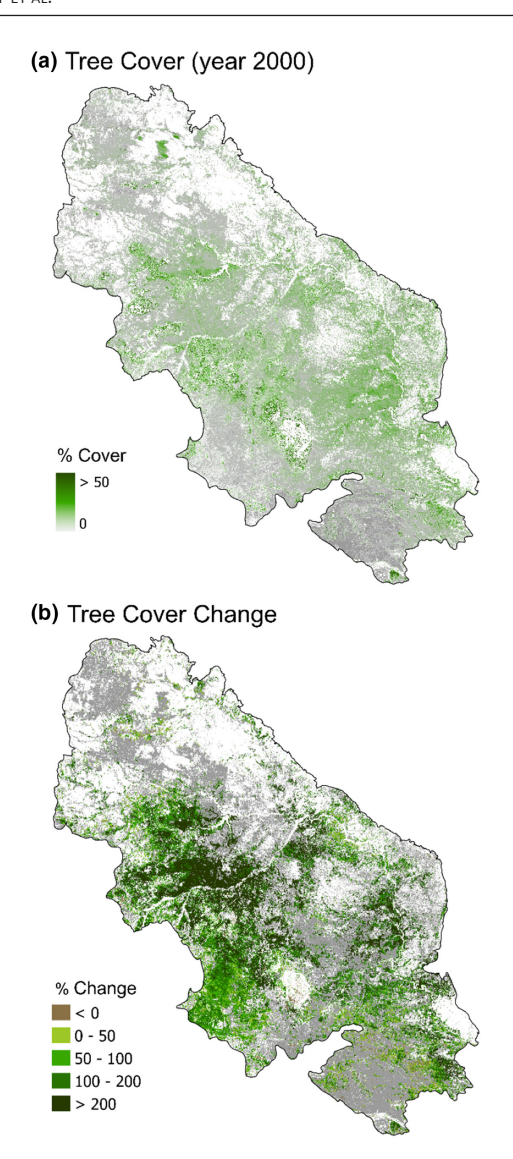


FIGURE 4 NGP grassland (shaded grey) tree cover and tree cover changes. (a) Percent tree cover from MODIS for the year 2000 and (b) the statistically significant proportional change between 2000 and 2019. White areas represent non-grasslands (i.e., forested, cropland, urban, wetland)

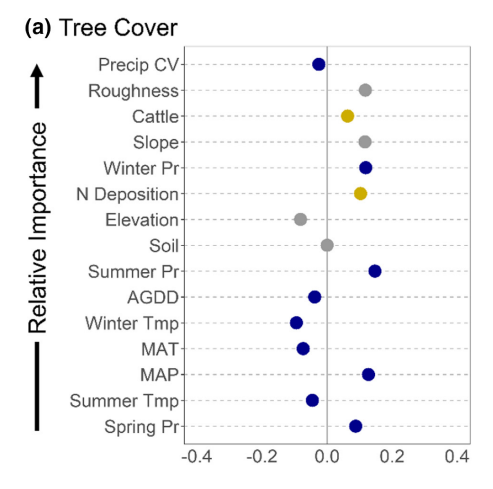
was 1.7% but increased to 4.7% over the two-decade period, signalling larger changes at higher tree cover densities (Table 2). Nonetheless, 2000 and 2019 tree cover had a large degree of spatial similarity (A = 0.79).

## 3.2.4 | Driving variables of tree cover and WPE

Models of both static percent tree cover and changing percent tree cover performed well, with an error of 1.6% for the year 2000 tree cover model, 0.9% for the 2019 tree cover model and 1.8% error for the changing tree cover model. Based on the random forest models, the 15 driving variables of 2000 tree cover explained 54.5% of the variation, and the 24 predictors for 2019 tree cover and tree cover change explained 39.3% and 32.8% of the variability, respectively.

Initial tree cover was concentrated in areas with high topographic roughness and steeper slopes, with low precipitation variability and high winter precipitation (Figure 5a). Drivers of tree cover in 2000 and 2019 were highly correlated ( $\rho=0.79$ ), although many of the changing climate variables became important to tree cover in 2019 (Figure S2.1b).

In contrast to year 2000 tree cover, tree cover change was primarily driven by high precipitation variability, the absence of fire and other disturbances, and occurred on smoother topographies with lower slopes (Figure 5b). All changing precipitation variables were positively associated with WPE, indicating that



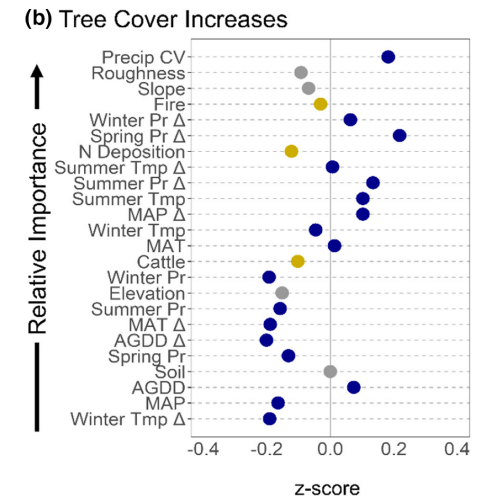


FIGURE 5 Relative importance from random forest models in descending order of importance for (a) percent tree cover (year 2000) and (b) tree cover percent increase. On the x-axis, standardized (z-score) effect size coefficients from ordinary least-squares regression. Positive values indicate a significant positive relationship with the tree cover metric; negative values indicate a significant negative relationship. Dots farther away from the zero line indicate a stronger directional relationship. The fire product was converted to a numeric variable, with positive values indicating fire presence. Soil is on the zero line as it was kept a categorical variable. Grey circles signify topographic variables, gold circles signify disturbance variables, and blue circles signify climate variables. Percent tree cover (a) has only variables that are relevant to the year 2000

the most significant proportional changes occurred where it has gotten wetter year-round. Finally, tree cover in 2000 and tree cover change had a low Tjøstheim coefficient (A = -0.11), and their respective drivers had a  $\rho$  = -0.52 Spearman correlation (Figure S2.1). This indicates that areas with the highest rates of WPE were not where tree cover was initially highest, nor were they associated with the same driving variables, emphasizing the point that tree cover change is occurring primarily as expansion rather than infilling.

# 3.3 | Concurrent greening and WPE

Both WPE and greening occurred across vast areas of NGP grass-lands. Here, we document that these changes were often concurrent and influenced by similar drivers. While 6.3%–12.7% of WPE and 23.0%–35.5% of greening occurred independent of one another (depending on which greening metric is examined in conjunction with WPE; i.e., WPE and LAI, WPE and peak NDVI, or WPE and mean NDVI), the largest proportion of vegetative changes were concurrent (Table 3).

This was particularly true for LAI and percent tree cover, which increased simultaneously across 40.6% of grasslands (Table 3, Figure S2.2a). A doubling of percent tree cover corresponded with a  $5.2\pm0.04\%$  increase in LAI (p<0.001), and WPE explained 11.1% of the variability in LAI greening. Indeed, we found a relatively strong spatial correlation (A = 0.49) and a very strong correlation between drivers of WPE and LAI ( $\rho$  = 0.67; Table S2.1).

We found similar results for NDVI variables; 34.1% of all grass-lands experienced increases in peak NDVI and WPE (Table 3, Figure S2.2b), and 34.2% underwent mean NDVI-based greening and WPE (Table 3, Figure S2.2c). For every doubling of percent tree cover, peak NDVI increased by  $1.28\pm0.01\%$  (p<0.001) and mean NDVI increased by  $0.91\pm0.01\%$  (p<0.001). WPE explained 9.7% of the variation in peak NDVI-based greening and 19.7% of mean NDVI increases. Interestingly, the Spearman correlation between drivers

TABLE 3 Percent of NGP grasslands undergoing synchronous versus mutually exclusive WPE and greening categorized by greening metric. As an example, 40.6% of NGP grasslands increased in LAI and tree cover synchronously. Conversely, 35.5% of the NGP experienced only LAI-based greening and 6.3% only WPE. Examining the *greening index and WPE*, we see that 19% of NGP grasslands increased in all three greening metrics and WPE

		Mutually exclusive		
Greening metric with WPE	Synchronous	Greening only	WPE	
LAI and WPE	40.6	35.5	6.3	
Peak NDVI and WPE	34.1	28.7	12.7	
Mean NDVI and WPE	34.2	23.0	12.6	
Greening Index and WPE	19.0	11.6	13.5	

of WPE and peak NDVI was the lowest ( $\rho=0.56$ ), suggesting that even though WPE and peak NDVI co-occurred across large areas, the primary drivers of each differed. Conversely, drivers of mean NDVI and WPE were highly correlated ( $\rho=0.76$ ), and both peak and mean NDVI had similar Tjøstheim's coefficients (A=0.43 and A=0.44, respectively, Table S2.1).

Finally, we document that 19.0% of NGP grasslands have simultaneously undergone increases in all three greening metrics and WPE (Figure 6a; Table 3). Greening and WPE were strongly and positively associated; a doubling of woody plant cover corresponded to a proportional 15.0% increase in the greening index (p<0.001; Figure 6b). Although WPE and the greening index were mutually exclusive across large portions of grasslands (Table 3), WPE explained 17.0% of the variability in the greening index across the NGP.

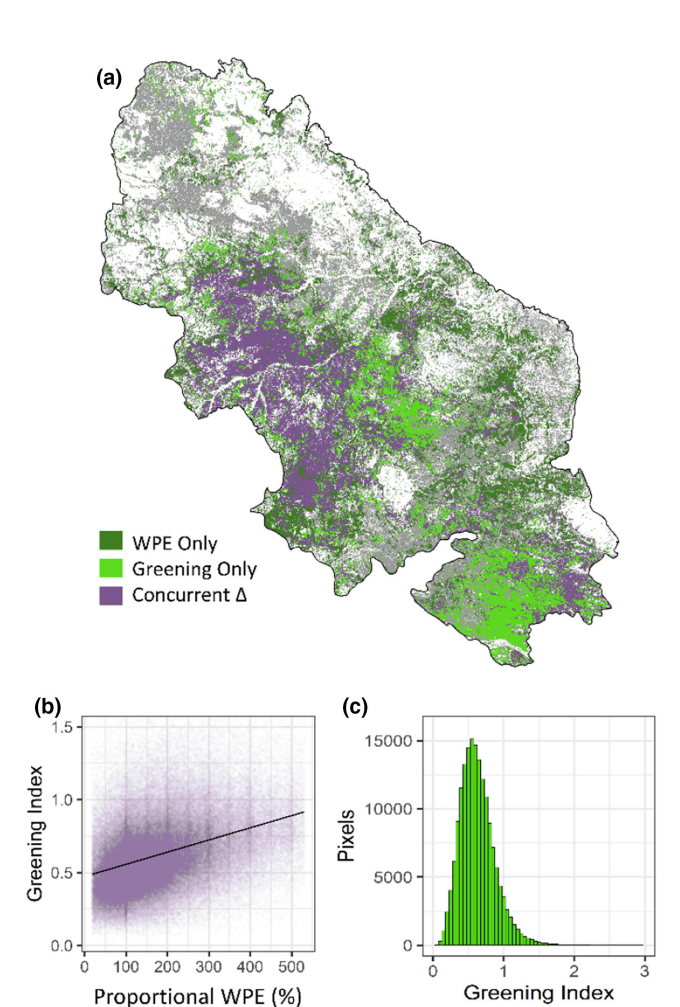


FIGURE 6 Greening and WPE across NGP grasslands (shaded grey; white areas represent non-grasslands). (a) Mapped changes. WPE only represents areas where only tree cover has increased. Greening only represents pixels where only greening has occurred. Greening is represented here as the 'greening index,' where peak NDVI, mean NDVI and LAI have increased simultaneously. Concurrent  $\Delta$  represents where greening and WPE have co-occurred. (b) Relationship between cells undergoing greening and concurrent tree cover increase. (c) Distribution of greening index values

# 4 | DISCUSSION

We document a strong coupling between WPE and vegetative greening at high-resolution (~500 m) across broad disturbance, climate and topographic gradients within one of the last remaining relatively intact high latitude grasslands globally. Significant increases in percent tree cover occur on smooth topographies and are primarily driven by the absence of fire and increasing temperature and precipitation. We demonstrate that a doubling in proportional tree cover drives a concurrent 15% proportional increase in our integrative greening index and that these synchronous vegetative changes occur across roughly one-fifth (roughly 90,000 km<sup>2</sup>) of all NGP grasslands. Indeed, WPE alone accounts for 17% of the variability in the greening index. Comparatively, all 24 other climatic, topographic and disturbance variables combined explained 17.4%-50.7% of the variance, depending on the greening metric. These results highlight that WPE is a large component of vegetative greening in the NGP and imply that it may be an underappreciated component of greening trends in other semi-arid biomes.

Our results provide necessary observations to benchmark and parameterize models of vegetation change over the next century. While our results point to a more tree-covered NGP in the future, observed rates of change are much lower than required to result in a fully forested NGP by 2100 suggested by some DGVM projections (Shafer et al., 2015). Despite large proportional changes in percent tree cover, absolute changes of percent tree cover across the NGP were small. Median percent tree cover increased by 1.8% over the two-decade period (~0.1% year<sup>-1</sup>), with the upper quartile showing a slightly larger increase of 3.8% (~0.2% year<sup>-1</sup>). A linear extrapolation of these trends suggests that WPE rates would have to increase more than fivefold to obtain full woody cover by end-of-century across the NGP (i.e., median tree cover of at least 50%).

Our analyses of recent WPE point to critical interactions between topography, fire and climate change in explaining the spatial distribution of this vegetative change. Early studies of vegetation distributions in the NGP observed that P. ponderosa and Juniperus spp. were historically restricted to fire-protected rocky scarps and uplands (Wells, 1965). In alignment with these findings, we show that initial (year 2000) tree cover was highest in rough terrain, yet the highest rates of WPE occurred on smooth terrain in the absence of fire. Furthermore, drivers of established tree cover in 2000 and subsequent vegetative changes differed, indicating that what once allowed for the establishment of trees is distinct from what is associated with their expansion and greening today. Although stand level stem dynamics cannot be determined at the spatial resolution used in this study, we find evidence that past tree cover and present WPE are negatively associated across space. This indicates that the majority of increasing percent tree cover is not where percent tree cover is currently the highest, providing evidence that trees are expanding. Facilitating this expansion was very low fire occurrence across the NGP, as less than 3% of NGP grasslands experienced fire over the 20-year period. Similar to the result of active fire suppression, the dominant fire regime across much of the NGP has shifted from one with a relatively frequent fire return interval (FRI) of <30–50 years to one of infrequent and small fires (e.g., > 50-year FRI; (Reid & Fuhlendorf, 2011; Umbanhowar, 1996). This trend could sustain WPE and greening further into the 21st century. It is also possible that, under a warming climate, higher woody fuel loads resulting from continued WPE could trigger novel vegetation-fire feedbacks characterized by more frequent high-intensity fire activity (Moritz et al., 2012).

Enhanced vegetative growth and WPE were strongly associated with spring and winter precipitation increases, with the highest proportional increases occurring in more arid areas characterized by high long-term precipitation variability and lower baseline productivity and tree cover. In fact, precipitation CV ranked as a more important driver than any other climate variables for all greening and tree cover change measures. These results are consistent with high precipitation sensitivity and higher marginal gains in vegetation growth in response to increasing water supply in more arid areas (Hoover et al., 2021; Hufkens et al., 2016; Ritter et al., 2020). The NGP has been getting wetter over the last few decades (Bromley et al., 2020; Polley et al., 2013) and is predicted to continue to get wetter in the future (Conant et al., 2018), a trend that may sustain increases in vegetative activity. At the same time, enhanced moisture stress associated with higher evaporative demand and continued declines in summer precipitation could potentially dampen greening and WPE trends.

Our documented greening rates of 0.2%-1.3% year<sup>-1</sup> align with climate-driven model simulations showing 20%-100% increases in NGP vegetative productivity over the next century (Hufkens et al., 2016; Reeves et al., 2014), but our results further suggest that shifts in vegetation composition and phenology may underlie some of these changes. While WPE has contributed disproportionately to greening relative to its spatial extent, enhanced vegetative productivity occurred across 23.0%-35.5% of NGP grasslands in the absence of WPE. This is likely in part due to an elongated growing season, consistent with the warming temperatures we observe in this study. Nonetheless, the fact that LAI and mean annual NDVI were strongly correlated with WPE suggests that increases in evergreen conifer cover enhance greening due to year-long photosynthetic activity and increased biomass. In contrast, peak NDVI had the lowest correlation with WPE, suggesting peak NDVI is largely driven by herbaceous-driven greening (Brookshire et al., 2020). Similarly, that peak NDVI had the lowest variance explained by climatological changes in our models may indicate that peak NDVI is more sensitive to interannual-to-annual climate variability than mean NDVI or LAI, both of which were better explained by our random forest models. These differences in model responses across greening variables highlight the importance of examining multiple greening metrics to capture the various aspects of phenology when examining greening phenomena of large-scale vegetative changes (Wood et al., 2021).

In addition to the elongation of photosynthetic activity associated with WPE, the increasing abundance of conifers raises important questions about potential shifts in plant resource acquisition

and use-efficiency that may affect future greening and WPE. Foliar isotope analysis shows that WUE of grassland vegetation across the NGP has increased by 37% on average since the 1960s in response to atmospheric CO<sub>2</sub> enrichment, while N availability has declined (Brookshire et al., 2020). Although declining N availability suggests a potential bottleneck to future greening, it also indicates enhanced NUE given sustained productivity. How coniferous WPE may affect these trajectories is less certain. For example, *P. ponderosa* and *Juniperus* spp. may have advantages over grasses in access to soil nutrients via differences in rooting depth or mycorrhizal nutrient acquisition strategies (Policelli et al., 2019) that could sustain tree expansion and greening, particularly under elevated CO<sub>2</sub> (Terrer et al., 2019).

Our machine learning approach highlights the challenges of using empirical modelling to benchmark process-based DGVM projections of vegetative changes. A notable disadvantage is a reliance on accurate and heterogeneous spatial data. For instance, atmospheric CO2 enrichment likely drives some of the patterns we observe through direct stimulation of photosynthesis and/or indirect enhancement of WUE and NUE (Brookshire et al., 2020), but we did not account for CO<sub>2</sub> due to its spatial homogeneity. In addition, although the MODIS VCF tree cover product has been validated across 442 WPE sites (Deng et al., 2021), this product has been shown to consistently underestimate tree cover by 0%-18% (Adzhar et al., 2022). Therefore, our estimates of WPE are conservative as we cannot capture trees too small or young to be included in the algorithm. Indeed, the WPE rate we document (~0.1% cover year<sup>-1</sup>) is lower than field estimates in other western North American grasslands (0.5%-0.6%, Barger et al., 2011), but closer to global estimates that use the same product (0.3% cover  $year^{-1}$ ; Deng et al., 2021).

Our findings document the pace of vegetation change and its dominant controls across one of the last remaining relatively intact grasslands worldwide and provide insight into alternative future ecosystem states. We have shown that the greening of the NGP is driven by interactions between large-scale vegetative shifts and cooccurring photosynthetic enhancement from established herbaceous vegetation. While recent WPE has contributed to enhanced C sequestration, WPE is also associated with a host of ecosystem and socio-economic tradeoffs, including loss of grassland biodiversity, transformation of biogeochemical cycles, and changes to wildlife habitat (Barger et al., 2011; Epstein et al., 2021; Symstad & Leis, 2017; Wilcox et al., 2018). Furthermore, the combination of higher conifer densities and a warmer climate dramatically increases the probability of large wildfires (McWethy et al., 2019; Moritz et al., 2012). As such, assessment of these large-scale and interactive vegetative changes should be disassociated from values-based ideologies regarding whether woody encroachment and greening are entirely beneficial or detrimental processes. Instead, it is important to examine the complex tradeoffs between these vegetative changes to guide understanding, evaluation and management of future vegetative states and functions under projected climate change.

#### **ACKNOWLEDGEMENTS**

We thank Simon Scheiter, Anping Chen and an anonymous reviewer for their insightful improvements to this manuscript. This work was supported by the National Science Foundation, Award Numbers: OIA-1632810 (ENJB) and BCS 1832486 (DBM), the Montana Agricultural Experiment Station and the Department of Interior, Bureau of Land Management award L16AS00082 to ENJB. No permits were required for this research.

#### **CONFLICT OF INTEREST**

The authors declare no conflict of interest.

#### DATA AVAILABILITY STATEMENT

All large datasets are in .csv format and are available on datadryad. org at 10.5061/dryad.z08kprrdj. All other datasets, code, and figures are publicly available on this project's repository on github.com at 10.5281/zenodo.6473246.

#### ORCID

Bryce Currey https://orcid.org/0000-0001-9794-9906

David B. McWethy https://orcid.org/0000-0003-3879-4865

E. N. Jack Brookshire https://orcid.org/0000-0002-0412-7696

#### REFERENCES

Adzhar, R., Kelley, D. I., Dong, N., George, C., Torello Raventos, M., Veenendaal, E., Feldpausch, T. R., Phillips, O. L., Lewis, S. L., Sonké, B., Taedoumg, H., Schwantes Marimon, B., Domingues, T., Arroyo, L., Djagbletey, G., Saiz, G., & Gerard, F. (2022). MODIS vegetation continuous fields tree cover needs calibrating in tropical savannas. *Biogeosciences*, 19(5), 1377–1394. https://doi.org/10.5194/bg-19-1377-2022

Andersen, E. M., & Steidl, R. J. (2019). Woody plant encroachment restructures bird communities in semiarid grasslands. Biological Conservation, 240, 108276. https://doi.org/10.1016/j.biocon.2019.108276

Archer, S. R., Andersen, E. M., Predick, K. I., Schwinning, S., Steidl, R. J., & Woods, S. R. (2017). Woody Plant encroachment: Causes and consequences. In D. D. Briske (Ed.), Rangeland systems: Processes, management and challenges (pp. 25–84). Springer International Publishing. https://doi.org/10.1007/978-3-319-46709-2\_2

Barger, N. N., Archer, S. R., Campbell, J. L., Huang, C., Morton, J. A., & Knapp, A. K. (2011). Woody plant proliferation in north American drylands: A synthesis of impacts on ecosystem carbon balance. *Journal of Geophysical Research Biogeosciences*, 116, G00K07. https://doi.org/10.1029/2010JG001506

Bromley, G. T., Gerken, T., Prein, A. F., & Stoy, P. C. (2020). Recent trends in the near-surface climatology of the northern north American Great Plains. *Journal of Climate*, 33(2), 461–475. https://doi.org/10.1175/JCLI-D-19-0106.1

Brookshire, E. N. J., Stoy, P. C., Currey, B., & Finney, B. (2020). The greening of the northern Great Plains and its biogeochemical precursors. *Global Change Biology*, 26(10), 5404–5413. https://doi.org/10.1111/gcb.15115

Brown, P. M., & Sieg, C. H. (1999). Historical variability in fire at the ponderosa pine—Northern Great Plains prairie ecotone, southeastern Black Hills, South Dakota. *Écoscience*, 6(4), 539–547. https://doi.org/10.1080/11956860.1999.11682563

Chen, C., Park, T., Wang, X., Piao, S., Xu, B., Chaturvedi, R. K., Fuchs, R., Brovkin, V., Ciais, P., Fensholt, R., Tømmervik, H., Bala, G., Zhu,

- Z., Nemani, R. R., & Myneni, R. B. (2019). China and India lead in greening of the world through land-use management. *Nature Sustainability*, 2(2), 122–129. https://doi.org/10.1038/s4189 3-019-0220-7
- Chen, M., Parton, W. J., Hartman, M. D., Grosso, S. J. D., Smith, W. K., Knapp, A. K., Lutz, S., Derner, J. D., Tucker, C. J., Ojima, D. S., Volesky, J. D., Stephenson, M. B., Schacht, W. H., & Gao, W. (2019). Assessing precipitation, evapotranspiration, and NDVI as controls of U.S. Great Plains plant production. *Ecosphere*, 10(10), e02889. https://doi.org/10.1002/ecs2.2889
- Conant, R. T., Kluck, D., Anderson, A., Badger, A., Boustead, B. M., Derner, J., Farris, L., Hayes, M. J., Livneh, B., McNeeley, S., Peck, D., Shulski, M. D., & Small, V. A. (2018). Northern Great Plains. *In Impacts, risks, and adaptation in the United States: Fourth National Climate Assessment*, Volume II (pp. 941-986). U.S. Global Change Research Program. https://doi.org/10.7930/NCA4.2018.CH22
- Criado, M. G., Myers-Smith, I. H., Bjorkman, A. D., Lehmann, C. E. R., & Stevens, N. (2020). Woody plant encroachment intensifies under climate change across tundra and savanna biomes. Global Ecology and Biogeography, 29(5), 925–943. https://doi.org/10.1111/ geb.13072
- Deng, Y., Li, X., Shi, F., & Hu, X. (2021). Woody plant encroachment enhanced global vegetation greening and ecosystem water-use efficiency. *Global Ecology and Biogeography*, 30(12), 2337–2353. https://doi.org/10.1111/geb.13386
- Eldridge, D. J., Bowker, M. A., Maestre, F. T., Roger, E., Reynolds, J. F., & Whitford, W. G. (2011). Impacts of shrub encroachment on ecosystem structure and functioning: Towards a global synthesis. *Ecology Letters*, 14(7), 709–722. https://doi.org/10.1111/j.1461-0248.2011.01630.x
- Epstein, K., Wood, D., Roemer, K., Currey, B., Duff, H., Gay, J., Goemann, H., Loewen, S., Milligan, M., Wendt, J., Brookshire, E. N. J., Maxwell, B., McNew, L., McWethy, D., Stoy, P., & Haggerty, J. (2021). Toward an urgent yet deliberate conservation strategy: Sustaining social-ecological systems in rangelands of the northern Great Plains, Montana. *Ecology and Society*, 26(10). https://doi.org/10.5751/ES-12141-260110
- Feng, Z., Rütting, T., Pleijel, H., Wallin, G., Reich, P. B., Kammann, C. I., Newton, P. C. D., Kobayashi, K., Luo, Y., & Uddling, J. (2015). Constraints to nitrogen acquisition of terrestrial plants under elevated CO2. Global Change Biology, 21(8), 3152–3168. https://doi.org/10.1111/gcb.12938
- Frank, D. A., McNaughton, S. J., & Tracy, B. F. (1998). The ecology of the Earth's grazing ecosystems. *Bioscience*, 48(7), 513–521. https://doi.org/10.2307/1313313
- Frank, D. C., Poulter, B., Saurer, M., Esper, J., Huntingford, C., Helle, G., Treydte, K., Zimmermann, N. E., Schleser, G. H., Ahlström, A., Ciais, P., Friedlingstein, P., Levis, S., Lomas, M., Sitch, S., Viovy, N., Andreu-Hayles, L., Bednarz, Z., Berninger, F., & Boettger, T. (2015).
  Water-use efficiency and transpiration across European forests during the Anthropocene. *Nature Climate Change*, 5(6), 579–583. https://doi.org/10.1038/nclimate2614
- Fuhlendorf, S. D., Engle, D. M., Kerby, J., & Hamilton, R. (2009). Pyric herbivory: Rewilding landscapes through the recoupling of fire and grazing. *Conservation Biology*, 23(3), 588–598. https://doi.org/10.1111/j.1523-1739.2008.01139.x
- Geremia, C., Merkle, J. A., Eacker, D. R., Wallen, R. L., White, P. J., Hebblewhite, M., & Kauffman, M. J. (2019). Migrating bison engineer the green wave. *Proceedings of the National Academy of Sciences of the USA*, 116(51), 25707–25713. https://doi.org/10.1073/pnas.1913783116
- Hoover, D. L., Lauenroth, W. K., Milchunas, D. G., Porensky, L. M., Augustine, D. J., & Derner, J. D. (2021). Sensitivity of productivity to precipitation amount and pattern varies by topographic position in a semiarid grassland. *Ecosphere*, 12(2), e03376. https://doi. org/10.1002/ecs2.3376

- Hufkens, K., Keenan, T. F., Flanagan, L. B., Scott, R. L., Bernacchi, C. J., Joo, E., Brunsell, N. A., Verfaillie, J., & Richardson, A. D. (2016). Productivity of north American grasslands is increased under future climate scenarios despite rising aridity. *Nature Climate Change*, 6(7), 710-714. https://doi.org/10.1038/nclimate2942
- Klemm, T., Briske, D. D., & Reeves, M. C. (2020). Potential natural vegetation and NPP responses to future climates in the U.S. Great Plains. Ecosphere, 11(10), e03264. https://doi.org/10.1002/ecs2.3264
- Knapp, A. K., Briggs, J. M., Collins, S. L., Archer, S. R., Bret-Harte, M. S., Ewers, B. E., Peters, D. P., Young, D. R., Shaver, G. R., Pendall, E., & Cleary, M. B. (2008). Shrub encroachment in north American grasslands: Shifts in growth form dominance rapidly alters control of ecosystem carbon inputs. *Global Change Biology*, 14(3), 615–623. https://doi.org/10.1111/j.1365-2486.2007.01512.x
- Knapp, A. K., Ciais, P., & Smith, M. D. (2017). Reconciling inconsistencies in precipitation-productivity relationships: Implications for climate change. New Phytologist, 214(1), 41-47. https://doi.org/10.1111/ nph.14381
- Köchy, M., & Wilson, S. D. (2001). Nitrogen deposition and forest expansion in the northern Great Plains. *Journal of Ecology*, 89(5), 807–817. https://doi.org/10.1046/j.0022-0477.2001.00600.x
- McWethy, D. B., Schoennagel, T., Higuera, P. E., Krawchuk, M., Harvey, B. J., Metcalf, E. C., Schultz, C., Miller, C., Metcalf, A. L., & Buma, B. (2019). Rethinking resilience to wildfire. *Nature Sustainability*, 2(9), 797–804.
- Moritz, M. A., Parisien, M.-A., Batllori, E., Krawchuk, M. A., Dorn, J. V., Ganz, D. J., & Hayhoe, K. (2012). Climate change and disruptions to global fire activity. *Ecosphere*, 3(6), art49. https://doi.org/10.1890/ ES11-00345.1
- Myneni, R. B., Hall, F. G., Sellers, P. J., & Marshak, A. L. (1995). The interpretation of spectral vegetation indexes. *IEEE Transactions on Geoscience and Remote Sensing*, 33(2), 481–486. https://doi.org/10.1109/36.377948
- Phillips, W. S., Walter, S., Shantz, H. L., & Homer, L. (1963). Vegetational changes in northern Great Plains: Photographic documentation. College of Agriculture, University of Arizona. https://repository. arizona.edu/handle/10150/297663
- Piao, S., Wang, X., Park, T., Chen, C., Lian, X., He, Y., Bjerke, J. W., Chen, A., Ciais, P., Tømmervik, H., Nemani, R. R., & Myneni, R. B. (2020). Characteristics, drivers and feedbacks of global greening. *Nature Reviews Earth & Environment*, 1(1), 14–27. https://doi.org/10.1038/s43017-019-0001-x
- Policelli, N., Bruns, T. D., Vilgalys, R., & Nuñez, M. A. (2019). Suilloid fungi as global drivers of pine invasions. *New Phytologist*, 222(2), 714–725. https://doi.org/10.1111/nph.15660
- Polley, H. W., Briske, D. D., Morgan, J. A., Wolter, K., Bailey, D. W., & Brown, J. R. (2013). Climate change and north American range-lands: Trends, projections, and implications. *Rangeland Ecology & Management*, 66(5), 493–511. https://doi.org/10.2111/REM-D-12-00068.1
- Ratajczak, Z., Nippert, J. B., & Collins, S. L. (2012). Woody encroachment decreases diversity across north American grasslands and savannas. *Ecology*, 93(4), 697–703. https://doi.org/10.1890/11-1199.1
- Reeves, M. C., Hanberry, B. B., Wilmer, H., Kaplan, N. E., & Lauenroth, W. K. (2020). An assessment of production trends on the Great Plains from 1984 to 2017. *Rangeland Ecology & Management*, 76(1), 165–179. https://doi.org/10.1016/j.rama.2020.01.011
- Reeves, M. C., Moreno, A. L., Bagne, K. E., & Running, S. W. (2014). Estimating climate change effects on net primary production of rangelands in the United States. *Climatic Change*, 126(3), 429–442. https://doi.org/10.1007/s10584-014-1235-8
- Reid, A. M., & Fuhlendorf, S. D. (2011). Fire Management in the National Wildlife Refuge System: A case study of the Charles M. Russell National Wildlife Refuge, Montana. *Rangelands*, 33(2), 17–23. https://doi.org/10.2111/1551-501X-33.2.17

- Ritter, F., Berkelhammer, M., & Garcia-Eidell, C. (2020). Distinct response of gross primary productivity in five terrestrial biomes to precipitation variability. *Communications Earth & Environment*, 1(1), 1–8. https://doi.org/10.1038/s43247-020-00034-1
- Scholtz, R., Fuhlendorf, S. D., & Archer, S. R. (2018). Climate-fire interactions constrain potential woody plant cover and stature in north American Great Plains grasslands. Global Ecology and Biogeography, 27(8), 936–945.
- Shafer, S. L., Bartlein, P. J., Gray, E. M., & Pelltier, R. T. (2015). Projected future vegetation changes for the Northwest United States and Southwest Canada at a fine spatial resolution using a dynamic global vegetation model. *PLoS One*, 10(10), e0138759. https://doi. org/10.1371/journal.pone.0138759
- Stevens, N., Lehmann, C. E. R., Murphy, B. P., & Durigan, G. (2017). Savanna woody encroachment is widespread across three continents. *Global Change Biology*, 23(1), 235–244. https://doi.org/10.1111/gcb.13409
- Symstad, A. J., & Leis, S. A. (2017). Woody encroachment in northern Great Plains grasslands: Perceptions, actions, and needs. *Natural Areas Journal*, 37(1), 118–127. https://doi.org/10.3375/043.037.0114
- Symstad, A. J., Smith, A. T., Newton, W. E., & Knapp, A. K. (2019). Experimentally derived nitrogen critical loads for northern Great Plains vegetation. *Ecological Applications*, 29(5), e01915. https://doi. org/10.1002/eap.1915
- Terrer, C., Jackson, R. B., Prentice, I. C., Keenan, T. F., Kaiser, C., Vicca, S., Fisher, J. B., Reich, P. B., Stocker, B. D., Hungate, B. A., Peñuelas, J., McCallum, I., Soudzilovskaia, N. A., Cernusak, L. A., Talhelm, A. F., Sundert, K. V., Piao, S., Newton, P. C. D., Hovenden, M. J., ... Franklin, O. (2019). Nitrogen and phosphorus constrain the CO<sub>2</sub> fertilization of global plant biomass. Nature Climate Change, 684-689. https://doi.org/10.1038/s41558-019-0545-2
- Umbanhowar, C. E. (1996). Recent fire history of the northern Great Plains. *The American Midland Naturalist*, 135(1), 115-121. https://doi.org/10.2307/2426877
- Wells, P. V. (1965). Scarp woodlands, transported grassland soils, and concept of grassland climate in the Great Plains region. *Science*, 148(3667), 246–249.
- Welti, E. A. R., Roeder, K. A., Beurs, K. M. de, Joern, A., & Kaspari, M. (2020). Nutrient dilution and climate cycles underlie declines in a dominant insect herbivore. *Proceedings of the National Academy of Sciences of the USA*, 117(13), 7271–7275. https://doi.org/10.1073/pnas.1920012117
- Wilcox, B. P., Birt, A., Fuhlendorf, S. D., & Archer, S. R. (2018).
  Emerging frameworks for understanding and mitigating woody plant encroachment in grassy biomes. Current Opinion in Environmental Sustainability, 32, 46–52. https://doi.org/10.1016/j.cosust.2018.04.005

- Wood, D. J. A., Powell, S., Stoy, P. C., Thurman, L. L., & Beever, E. A. (2021). Is the grass always greener? Land surface phenology reveals differences in peak and season-long vegetation productivity responses to climate and management. *Ecology and Evolution*, 11(16), 11168–11199. https://doi.org/10.1002/ece3.7904
- Xiao, J., & Moody, A. (2005). Geographical distribution of global greening trends and their climatic correlates: 1982–1998. *International Journal of Remote Sensing*, 26(11), 2371–2390. https://doi.org/10.1080/01431160500033682
- Zhu, Z., Piao, S., Myneni, R. B., Huang, M., Zeng, Z., Canadell, J. G., Ciais, P., Sitch, S., Friedlingstein, P., Arneth, A., Cao, C., Cheng, L., Kato, E., Koven, C., Li, Y., Lian, X., Liu, Y., Liu, R., Mao, J., ... Zeng, N. (2016). Greening of the earth and its drivers. *Nature Climate Change*, 6(8), 791–795. https://doi.org/10.1038/nclimate3004

#### BIOSKETCH

Bryce Currey is a PhD candidate at the Montana State University. Broadly, his work focuses on ecological and biogeochemical dynamics across multiple scales. By employing tools from classic field ecology and remote sensing, his research examines the properties and dynamics that emerge at larger landscape scales, and how these dynamics scale or change when compared with finer-scale in-situ observation. The ecosystems that he currently conducts research in include tropical forests, temperate grasslands and temperate savannas.

Author contributions: B.C., E.N.J.B. and D.B.M. conceived and designed the study. N.R.F. handled the soils' data. B.C. conducted all analyses and wrote the first edition of the manuscript. All authors contributed to the revision of the manuscript.

#### SUPPORTING INFORMATION

Additional supporting information may be found in the online version of the article at the publisher's website.

How to cite this article: Currey, B., McWethy, D. B., Fox, N. R. & Brookshire, E. N. (2022). Large contribution of woody plant expansion to recent vegetative greening of the Northern Great Plains. *Journal of Biogeography*, 00, 1–12. https://doi.org/10.1111/jbi.14391